Active

Project #: E-21-Z78 Cost share #: Rev #: 3
Center # : 10/24-6-R8677-0A0 Center shr #: OCA file #:
Work type : RES
Contract#: AGREEMENT DATED 950908 Mod #: 1 Document : AGR
Prime #: Contract entity: GTRC

Subprojects ? : N CFDA:
Main project #: PE #:

Project unit: ECE Unit code: 02.010.118
Project director(s):
BRENNAN K ECE (404)894-6767

Sponsor/division names: ITT /
Sponsor/division codes: 208 / 023

Award period: 950912 to 960615 (performance) 960615 (reports)

Sponsor amount	New this change	Total to date
Contract value	0.00	27,628.00
Funded	0.00	27,628.00
Cost sharing amount		0.00

Does subcontracting plan apply ?: N

Title: FEASIBILITY STUDY OF INTEGRATED SUPERLATTICE APDS AND APS AS POTENTIAL...

PROJECT ADMINISTRATION DATA

OCA contact: Anita D. Rowland 894-4820

Sponsor technical contact	Sponsor issuing office
CHIP HAMBRO (703)563-0371	PEGGY V. CREASY (703)362-7330
ITT 7635 PLANTATION ROAD ROANOKE, VIRGINIA 24019	SAME

Security class (U,C,S,TS) : U ONR resident rep. is ACO (Y/N): N
Defense priority rating : supplemental sheet
Equipment title vests with: Sponsor GIT
N/A
Administrative comments -
MODIFICATION NO. 1 EXTEDNS PERIOD THRU 6.15.96

GEORGIA INSTITUTE OF TECHNOLOGY
OFFICE OF CONTRACT ADMINISTRATION

NOTICE OF PROJECT CLOSEOUT

Closeout Notice Date 06/18/96

Project No. E-21-Z78_____ Center No. 10/24-6-R8677-0A0_

Project Director BRENNAN K_____ School/Lab ECE_____

Sponsor ITT/_____

Contract/Grant No. AGREEMENT DATED 950908_____ Contract Entity GTRC

Prime Contract No. _____

Title FEASIBILITY STUDY OF INTEGRATED SUPERLATTICE APDS AND APS AS POTENTIAL...

Effective Completion Date 960615 (Performance) 960615 (Reports)

Closeout Actions Required:	Y/N	Date Submitted
Final Invoice or Copy of Final Invoice	Y	_____
Final Report of Inventions and/or Subcontracts	Y	_____
Government Property Inventory & Related Certificate	N	_____
Classified Material Certificate	N	_____
Release and Assignment	N	_____
Other _____	N	_____

Comments_____

Subproject Under Main Project No. _____

Continues Project No. _____

Distribution Required:

Project Director	Y
Administrative Network Representative	Y
GTRI Accounting/Grants and Contracts	Y
Procurement/Supply Services	Y
Research Property Managment	Y
Research Security Services	N
Reports Coordinator (OCA)	Y
GTRC	Y
Project File	Y
Other _____	N
_____	N

NOTE: Final Patent Questionnaire sent to PDPI.

E-21-278

#1

Final Report
Georgia Institute of Technology
ITT Image Intensifier Project

Title: Feasibility study of integrated superlattice avalanche photodiodes and active pixel sensors as potential image intensifiers

Senior Investigator: Dr. Kevin F. Brennan, Professor and Institute Fellow

Telephone: (404) 894-6767

Address: School of Electrical and Computer Engineering
Georgia Institute of Technology
Atlanta, Georgia
30332-0250

Email: kbrennan@ee.gatech.edu

Fax: (404) 894-1256

Abstract

It is found that a silicon reach through avalanche photodiode, RAPD, device can operate under all low light level imaging conditions (overcast, moonless conditions) in principal provided that the dark current arising from Shockley-Read-Hall, SRH, generation can be controlled to a level corresponding to 1 sec generation lifetimes. A numerical simulation of a RAPD device is made using an advanced drift-diffusion/hydrodynamic simulator. Our calculations indicate that a silicon RAPD having an absorption thickness of ~ 50 μm, an exhibiting a gain of ~20, can also provide sufficient signal to overcome the readout noise of existing, uncooled, silicon CCDs. The collected charge is then stored within the depletion region of the RAPD and can be readout either into a CCD or an APS array. Again, if the SRH lifetime is ~1 sec, the RAPD can store the signal charge without serious degradation for up to 10-30 msec. If the light level is somewhat relaxed, corresponding to a clear, moonless night, then the RAPD will operate even if the SRH generation lifetimes cannot be increased beyond ~ 1msec.

I. Introduction

One of the key developments in modern surveillance operations is the capability to operate under limited visual conditions such as darkness, fog, rain, smoke, etc. Two distinct modalities have been developed for sensing in the dark. The first method operates by amplifying the ambient optical and near infrared radiation to produce an image. This technique is called image intensification and the devices which are used to perform this function are called image intensifiers. The second method relies on thermal imaging. In this technique the heat emitted by an object is collected and converted into an image (thermal contrast is converted into visual contrast on a display). Thermal imaging relies on the collection of far longer wavelength radiation than image intensification and can be used during both day and night.

Thermal imagers provide far better imaging through smoke, fog and rain than do image intensifiers. This is due to the fact that thermal radiation is emitted at much longer wavelengths, ~ 3- 14 microns, longer typically than the dimensions of smoke, fog or rain particles within the air, and is consequently not strongly scattered by the particles. Additionally, thermal imagers can detect objects at far greater distances than image intensifiers [1]. Subsequently, for long range, full day/night/foul weather applications a thermal imaging system is superior to an image intensifier. However, image intensification is of primary importance in piloting, maneuvering, reconnaissance and surveillance where the operator needs to be able to distinguish between objects with the same temperature signature. For example, an image intensifier enables a user to discern rocks, tree stumps, wires, holes, etc. while walking or driving at night.

Image intensifiers amplify the ambient background light. Even though in darkness with no moon where there is little ambient optical radiation present, there is still near visible, near infrared radiation. The sources of this radiation are zodaical light and airglow. Zodaical light originates from solar radiation scattered by residual interplanetary dust within the orbital plane. Airglow is caused by excitation of atoms and molecules in the upper atmosphere that are heated by the sun during the day and then release this energy at night. While the radiation produced by airglow and zodaical light cannot be seen by the unaided eye, this radiation can be used by image intensifiers as a source of illumination. Typically, airglow and zodaical radiation provide an illuminance an order of magnitude higher than starlight alone [2].

The most demanding applications for low light level imaging are typically military in nature. However, there are emerging commercial applications for all weather imaging. These include search and rescue, law enforcement, fire fighting, and civilian piloting on the ground, sea and air. Of particular interest is the usage of image intensification as a nighttime driving aid owing to the large potential market. For commercial nighttime driving, the light level of operation is significantly brighter than that available for military operations, since headlight illumination is available.

It is thought that an image intensification system can be added to an automobile to serve as a driving aid. The output from the image intensifier will be shown on a flat panel display that the driver can glance at occasionally while driving, much like a rearview mirror is used today. In addition, to image intensified data, the flat panel display might also show the present location of the vehicle, its course as well as instructions for reaching its

destination. The system will require the capability of fusing information from multiple sources, i.e., image intensified data, global positioning satellite (GPS) data, stored map data, etc. Digitization of these data sources is then essential. Subsequently, the image intensifier system must produce an electronic digital output which can then be redisplayed or fused with other information prior to being displayed.

To date, the most successful image intensifier platform utilizes tube technology. These devices are collectively referred to as the GEN III image intensifier tubes. These tubes consist of three main components, a photocathode, a microchannel plate, MCP,and an output light phosphor as shown in Figure 1. The tube is of course in high vacuum and requires high voltage for operation. Photons are incident onto the semitransparent photocathode where they are converted into electrons. The electrons are then emitted into the vacuum by the photocathode and are accelerated by an electric field into the MCP channels. The electrons accelerate to high energies through the MCP channels. During the course of the electrons flights through the MCP channels, they suffer substantial collisions with the sides resulting in the production of numerous secondary electrons providing signal gain. Depending upon the applied voltage, efficiency and size of the MCP, one incident electron can lead to the ultimate generation of ~1000-3000 descendants [3]. Upon exiting the MCP, the electrons are accelerated again through vacuum under the influence of another electric field towards a phosphor screen. After striking the phosphor screen, the electrons are converted back into photons resulting in a greatly amplified optical image. In most designs, the gap between each component is very small such that there is little lateral drift of the electrons. Consequently, an image focussed onto the photocathode is correctly reproduced on the phosphor screen. This arrangement is

called proximity focus. Finally, the output image must be inverted since the input objective lens produces an upside down image at the tube input. Image inversion is typically obtained using a fiber-optic invertor [3] known as a twister. Alternative designs utilize electrostatic inverting electron lenses between the photocathode and the MCP for image inversion [4]. Sketches of the these two design types are shown in Figure 2.

One of the primary difficulties in transfering the GEN III image intensifier tubes to commercial driving applications is the fact that the tubes produce a photonic output rather than an electronic one. Consequently, for redisplaying information, a standard GEN III tube is unsatisfactory.

An electronic output can be obtained by fitting a GEN III tube to a charge coupled device, CCD. Two of the most promising means of using CCDs for image intensification are either optically coupling the CCD to the phosphor screen of an existing tube using an objective or a fiber optic plate, or inserting the CCD in place of the phosphor screen and directly bombarding it with electrons [5-7]. Usage of CCDs in these modes does not circumvent the limitations of the tubes in terms of cost, size and weight since these devices are again vacuum devices which incorporate all or some of the tube components. Nevertheless, these CCD designs provide an electronic output which can be digitized to provide data integration.

The CCD can be directly applied to low light level imaging, but this typically requires cryogenic cooling, slow scan readout rates, and extended integration times [8]. In any event, direct application of a CCD in low light level imaging requires back illumination, which necessitates in turn extensive wafer thinning. The main limitation in using CCDs

directly in low light levels is that in their simplest implementation, they do not provide any front end gain. Subsequently, in order to collect sufficient carriers to overcome readout noise, etc. the integration time of the CCD must be extended resulting in slower readout rates. In fact, for very low light levels, insufficient carriers are collected to overcome the noise floor in a typical room temperature operated CCD. For these reasons, the direct usefulness of the currently available CCDs is restricted in low light level applications. However, if the readout noise can be further suppressed or if the incident light signal level is relatively high, gain is not necessarily required for low light level CCD operation. In this report, we examine the conditions under which a back illuminated CCD can be used directly in low light level imaging.

Another approach to directly using CCDs requires their modification to provide front end gain. By inserting an avalanche photodiode, APD, array on top, a CCD can be effective in low light level imaging. An APD is a photodiode sufficiently reverse biased such that carrier multiplication via impact ionization occurs. Incident light is absorbed within the photodiode and the subsequently photogenerated carriers are multiplied through impact ionization events. The carrier multiplication provides gain. The multiplied carriers are collected within the depletion layer of the APD, and are transfered into the CCD wells for readout after a suitable integration time. By combining the amplification of the APD array with the CCD readout, ultra-low light level imaging is possible.

Additionally, an APD can be integrated with an active pixel sensor, APS, device. APS devices have numerous advantages over CCDs, principally arising from the fact that charge transfer occurs in an APS device only between two gates rather than completely across

a chip as in CCDs. An APD array can be readily bump bonded to either a CCD or an APS chip. However, it is possible to integrate an APD within the same chip as APS circuitry, while it is far more challenging to integrate APDs within the same chip as a CCD.

II. Need for Gain in Solid State Low Light Level Imaging Applications

In order to assess the gain requirement for low light level imaging, we have performed some simulations of a simple photodiode structure. From our previous report, it was determined that gain stretches the light level coverage for CCD operation. In that report, however, we only performed relatively rough calculations making a number of assumptions and utilizing simplified analytical models. Here we present new results based on the simulation of the effects of illumination of a silicon reach through avalanche photodiode, (RAPD), device. The silicon RAPD device is somewhat similar to a silicon CCD except it offers the additional advantage of providing gain if desired. A sketch of the structure is shown in Figure 3. The device is illuminated from the p+ side. Below the p+ layer is an intrinsic silicon layer measuring 46.5 μm in length, followed by a p layer and finally an n+ layer. Upon biasing, the p layer ultimately becomes fully depleted, and a high electric field is formed between the n+ and p layers. The field profile then consists of a relatively small field within the intrinsic layer, followed by a very high field, which if sufficiently biased, can provide carrier multiplication through impact ionization. The effective collection area is assumed to be 24 x 24 μm^2. The device is initially biased to 60 V and is then open circuited. The device slowly relaxes back to equilibrium from the action of the illuminated and dark generation rates within the reverse biased diode.

The simulations are performed using our advanced hydrodynamic simulator,

STEBS2D, but with only the drift-diffusion solver activated. We have found that the drift diffusion solver adequately models the behavior of standard and large sized photodiodes. For this reason and the fact that the parameters needed to correctly specify the hydrodynamic simulator are not accurately known nor accurately extractable at present, we perform all of the calculations presented here with our drift-diffusion solver. A ~8.3 msec integration time is chosen for the calculations since this yields a frame rate of about 120 frames/sec which is recommended for piloting applications.

Different Shockley-Read-Hall (SRH) generation lifetimes were chosen for this study. The longest SRH generation lifetime chosen was 1 second. A generation lifetime of 1 second corresponds to the highest quality silicon material available. We made additional calculations using different SRH lifetimes as discussed below. All of the other parameters used in the simulations, i.e., mobilities, diffusivities, etc. were standard and were taken from a commercial simulation package entitled, PC-1D.

The input light intensity was varied between two different extremes. The low light level was specified for a moonless, overcast night. The spectrum for the sky under these conditions is shown in Figure 4, and will be referred to as the EVC spectrum (for Electric Valve Corp. that performed the measurements [8]). At the other extreme, we consider an illumination of 1 Sun at 1.5 atm [9]. The 1 Sun spectrum is shown in Figure 5. We choose a very bright illumination to show the device's blooming characteristics.

The total charge stored as a function of illumination time for the reverse biased RAPD of Figure 3 is shown in Figure 6. Two different conditions are examined, with and without gain. Notice that in the absence of gain, which is the condition for a back illuminated CCD of

comparable collection width, that only ~ 20 electrons are collected in 8.3 msec. Given that the mean readout noise for a state-of-the-art CCD at room temperature operation is about 40 electrons, insufficient charge is collected to overcome the readout noise. It should also be noted that the collection layer width of back illuminated CCDs is significantly thinner than the collection layer width used here. In most CCDs, since there is very little field away from the surface, usage of a thicker absorber layer results in substantial lateral diffusion causing in turn interpixel blooming. Therefore, the actual number of electrons collected in a CCD given the EVC spectrum will most probably be significantly less than that predicted here using the RAPD. Subsequently, in order to effectively operate at very low illumination levels, a CCD would require either a significant reduction in readout noise or front end gain.

We have also determined the amount of charge collected given a gain of ~19. In this case after an 8.3 msec integration time, the total amount of collected charge is ~375, far greater than that necessary to overcome the readout noise of a CCD. Therefore, gain enables ultra-low light level detection in solid state imaging.

We further explored the effect of varying the generation lifetime on the amount of charge collected in the APD. For simplicity, we only consider generation processes from SRH centers located within the diode and neglect any surface state contribution to the generation rate. Charge generated from the SRH centers will be multiplied if the device exhibits multiplicative gain. We have found that for a lifetime of 1 sec, that the dark current is completely negligible without gain over an integration period of ~10 msec. Therefore, we investigate the case with gain. The total stored charge as a function of time assuming the same gain as in Figure 6 and without any input signal is plotted in Figure 7 for various

generation lifetimes. Different amounts of collected charge between the cases with very long lifetimes and short lifetimes arises from the much higher generation rate in the short lifetime cases. As the lifetime decreases, the amount of charge generated out of the SRH centers and later collected within the APD increases substantially. Again consider the condition after ~10 msec. From Figure 7 it can be seen that the total stored charge increases by roughly an order of magnitude with each order of magnitude decrease in the generation lifetime. The important finding determined from Figure 7 then is that the multiplied dark current arising solely from SRH processes at generation lifetimes less than or equal to 10 msec is appreciable. By comparing the multiplied dark currents shown in Figure 7 to the multiplied signal current shown in Figure 6, it is clear that even at a lifetime of 100msec, the dark current is roughly comparable to the multiplied EVC spectrum signal. ***Subsequently, almost perfect silicon material must be made, with a generation lifetime equal to the best measured performance to date, in order to detect the lowest signal level corresponding to an overcast, moonless night.***

It should be further noted however, that if the input spectrum is somewhat brighter, for instance that corresponding to the RCA data [10] which applies for a moonless, clear night, that the signal is sufficiently large that the dark currents do not limit performance until the SRH lifetime is severely degraded. We have calculated the response of the RAPD to the RCA illumination spectrum. It is found that the total collected charge exceeds 30,000 electrons in 10 msec. Examination of Figure 7 shows that the total collected charge due to the SRH multiplied dark current is significantly less than this amount if the generation lifetime is 1 msec or greater. ***Therefore, it is expected that a silicon based detector has sufficiently low dark current to operate under all night viewing conditions provided that the SRH generation***

lifetime is not less than ~1 sec. Provided there exists no cloud cover, a silicon based detector can operate provided the SRH generation lifetime is not less than 1 msec.

It is also interesting to examine the recovery time of the RAPD under an illumination corresponding to the EVC spectrum. The reverse voltage as a function of time is plotted in Figure 8. Recall that the device is initially reverse biased at t=0. It is then illuminated and begins to recover back to equilibrium. As can be seen from Figure 8, the reverse recovery time is extremely long given the EVC spectrum illumination. Notice that the decay is essentially linear during the 10 msec simulation time. This is because the amount of charge collected is extremely small. Subsequently, the voltage decays almost immeasurably.

For comparison, we also examine the behavior of the RAPD under bright illumination, that corresponding to 1 SUN at 1.5 atm (1.5 atm. is chosen to represent an acute angle of incidence). The reverse voltage as a function of time is plotted in Figure 9 for the RAPD at 1 SUN illumination. As can be seen from the figure, the voltage decays with two different timescales. The first decay is extremely rapid, where the voltage drops from over 70 volts to about 35 volts in ~2 ns as can be seen from the inset of Figure 9. This decay corresponds to the condition where the initial collected charge is multiplied. Notice that very little photogenerated charge results in a dramatic change in the voltage. This is due to the fact that the multiplication process produces a considerable amount of collected charge greatly lowering the voltage across the device. The second decay is far more gradual and arises from the collection of unmultiplied charge. As can be seen from the Figure, it takes roughly 1.5 μs for the device to recover back to equilibrium. Continued illumination results in a forward biasing of the diode as in a solar cell. It is expected that such behavior will lead to blooming

in the array.

In order to assess the sensitivity of the RAPD to variations in its dimensions, we make the following calculations. The most important parameter which can be readily altered is the thickness of the intrinsic region and hence the absorption layer thickness. It should be noted that the doping concentrations cannot be altered significantly since the device must be designed such that the p layer is fully depleted. Again an incident illumination corresponding to the EVC spectrum is assumed. For the RAPD shown in Figure 3, 44% of the incident photons are collected. If the intrinsic region is widened considerably such that the entire thickness of the RAPD is 200 μm, then 63% of the incident photons are collected. Though there is an increase in the percentage of photons collected of almost 43%, it comes at the possible expense of increased lateral diffusion between pixels. It is important to recognize that the thicker the absorbing layer becomes, the more likely photogenerated carriers will laterally diffuse to adjacent pixels, thereby smearing the image. Future calculations will be performed to quantitatively assess this effect. For now it should be noted that increasing the absorbing layer thickness does not necessarily improve the performance of the device.

III. Conclusions

From the above calculations, we recognize that a silicon RAPD device can operate under all low light level imaging conditions in principal provided that the dark current arising from SRH generation can be controlled to a level corresponding to 1 sec generation lifetimes. Generation lifetimes of 1 sec have been realized in silicon, but represent the best lifetimes measured to date. Our calculations indicate that a silicon RAPD having an absorption thickness of ~ 50 μm, an exhibiting a gain of ~20, can also provide sufficient signal to

overcome the readout noise of existing, uncooled, silicon CCDs. The collected charge is then stored within the depletion region of the RAPD and can be readout either into a CCD or an APS array. Again, if the SRH lifetime is ~1 sec, the RAPD can store the signal charge without serious degradation for up to 10-30 msec.

References

[1] E. N. Philips, "Electro-Optics - Image Intensifiers", ITT Internal Report, pp. 1-19, Doc: JSI/100, ITT Defense, Roanoke, VA.

[2] E. N. Philips, "Range performance analysis of image intensifier systems," ITT Internal Report, ITT Defense, Roanoke, VA.

[3] C. F. Freeman, "Image intensifier tubes," Applications of Electronic Imaging Systems, SPIE, vol. 143, pp. 3-13, 1978.

[4] Roy H. Holmes, "Night vision 94 Image Intensifiers", ITT Internal Report, ITT Defense, Roanoke, VA. , 1994.

[5] W. Enloe, R. Sheldon, L. Reed, and A. Amith, "An electron bombarded CCD image intensifier with a GaAs photocathode," SPIE vol. 1655, Electron Tubes and Image Intensifiers, pp. 41-49. 1992.

[6] J. C. Richard and R. Lemonier, "Intensified CCD's for low light level imaging," International Electronic Imaging Exposition and Conference, pp. 13-16, 1986.

[7] T. F. Lynch, "Development of intensified charge-coupled devices (CCDs) and solid state arrays," SPIE vol. 143, Applications of Electronic Imaging Systems, pp. 36-41, 1978.

[8] J. R. Howorth, "Night vision systems of the future using 1-2 μm," Proceedings of the IEE, Low Light and Thermal Imaging, 173, pp. 61-62, 1975.

[9] M. A. Green, Solar Cells, Prentice Hall, Englewood Cliffs, N. J., 1982.

[10] R. W. Engstrom and R. L. Rodgers, 3rd, "Camera tubes for night vision," Optical Spectra, pp. 26-30, Feb. 1971.

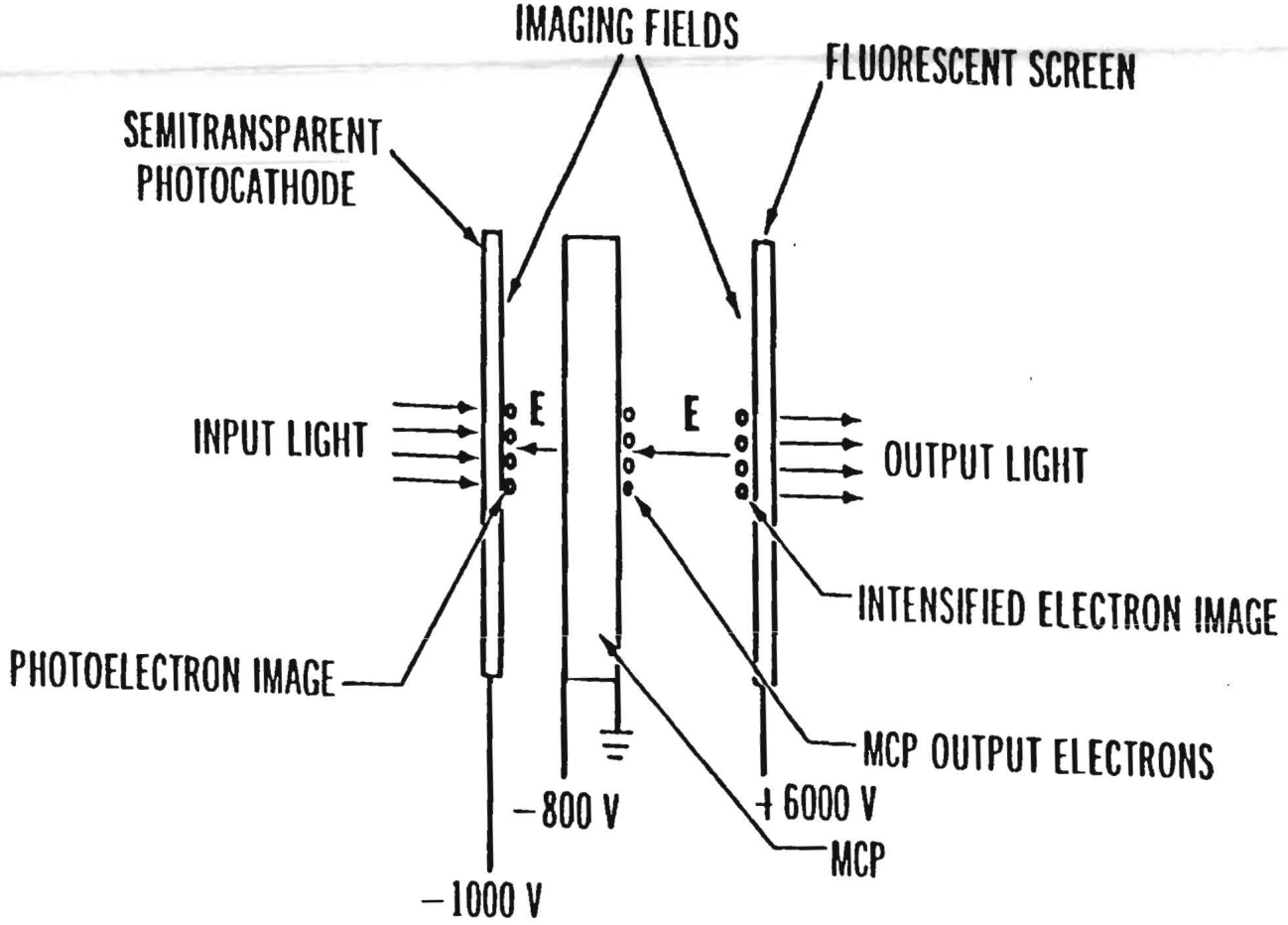

Figure 1: Basic tube anatomy for GEN II and GEN III image intensifier tubes.

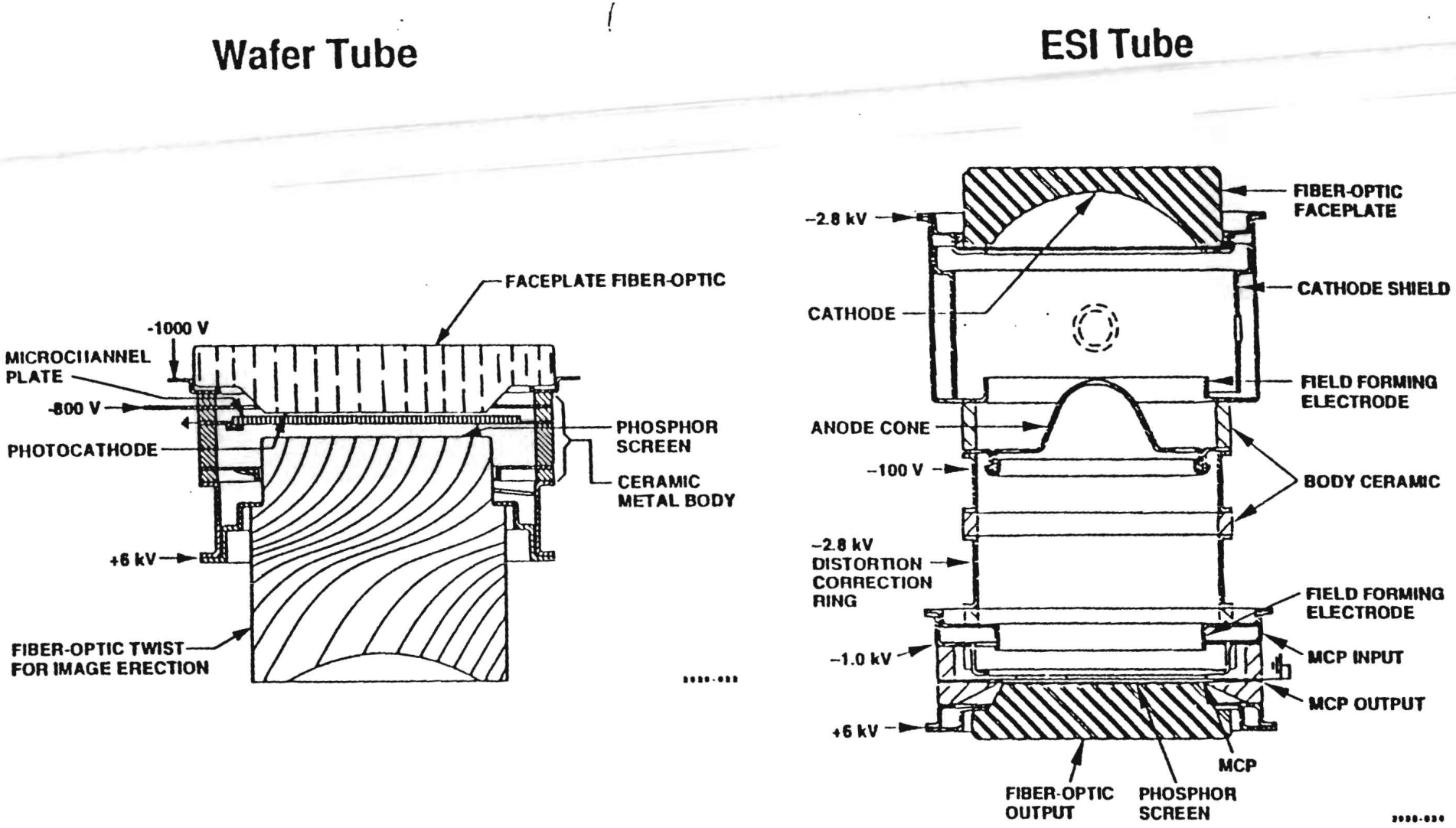

Figure 2: Sketches of fiber optic and electrostatic focusing GEN II tubes.

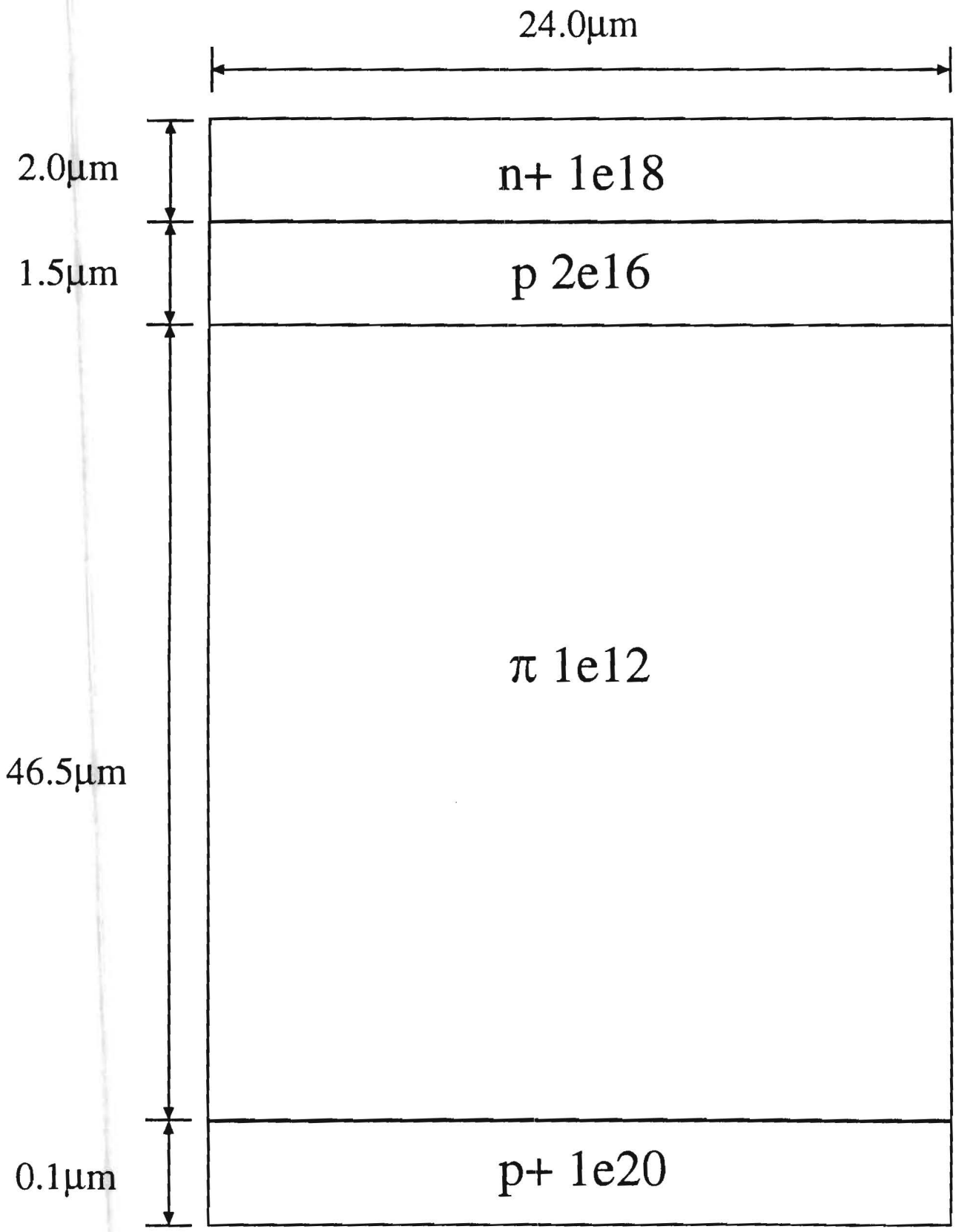

Fig 3. Reach Through APD Used for Reverse Recovery Calculations

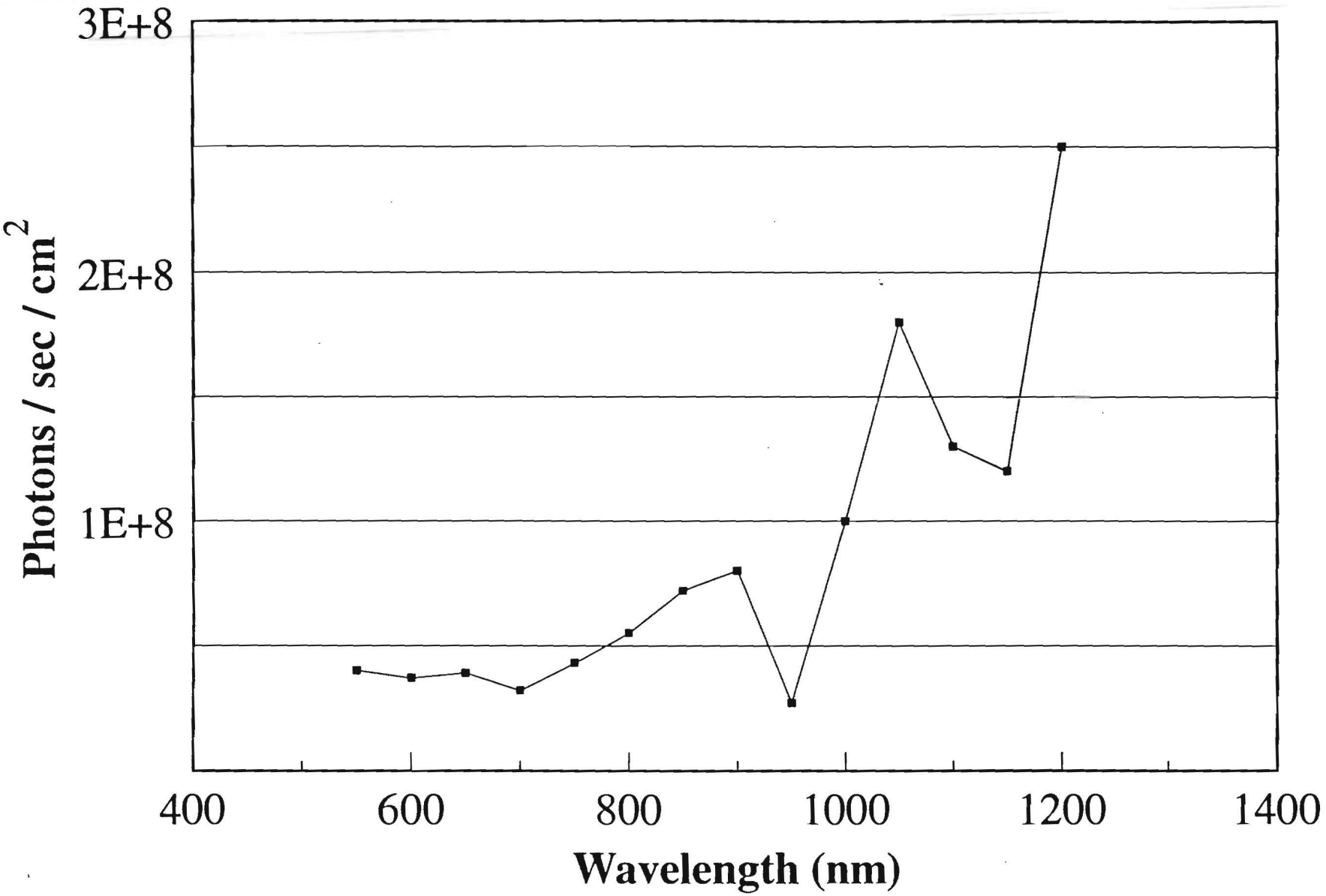

Fig 4. Night Sky Incident Radiation in Overcast Conditions

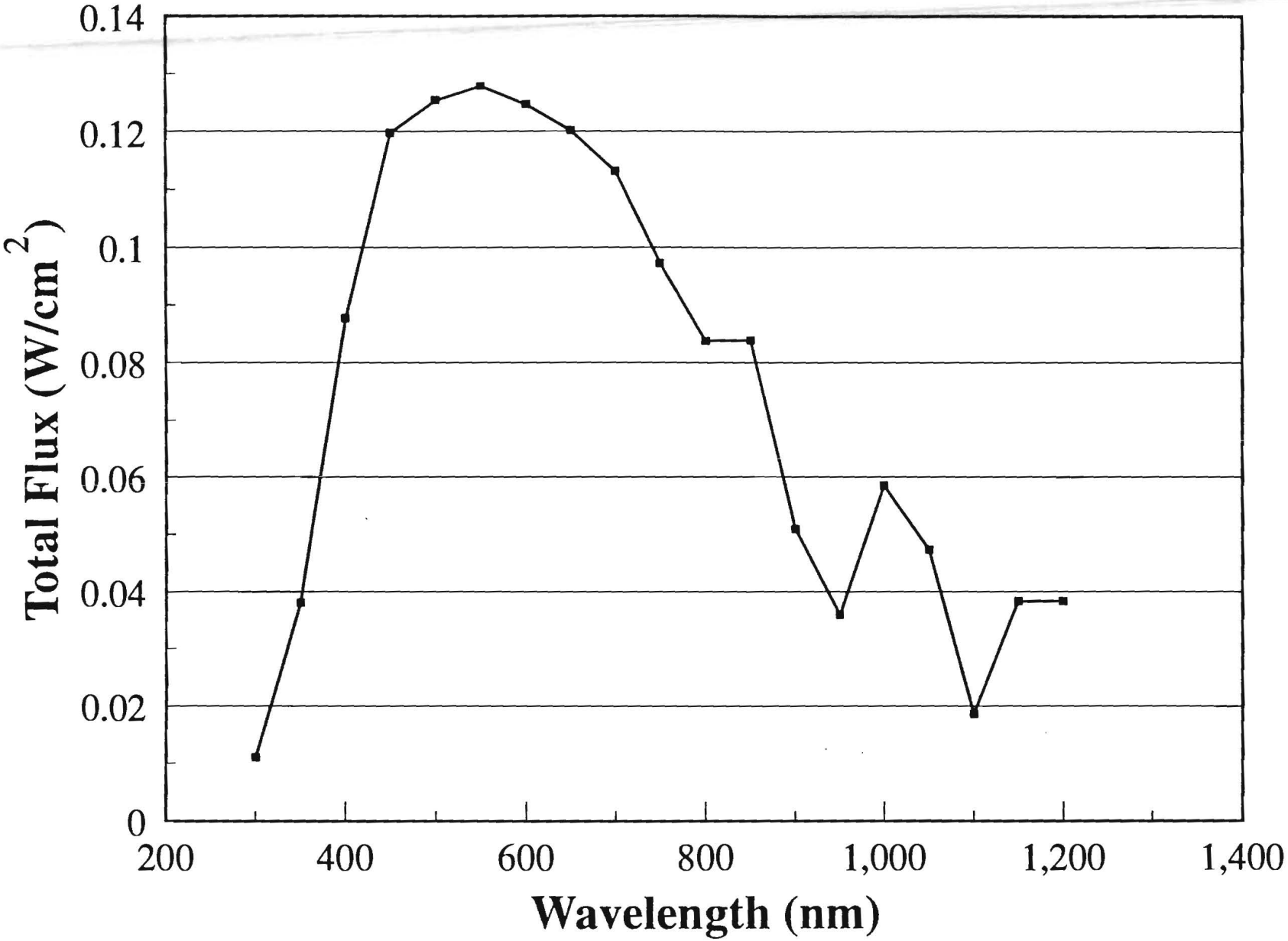

Fig 5. 1 Sun Spectrum at AM 1.5

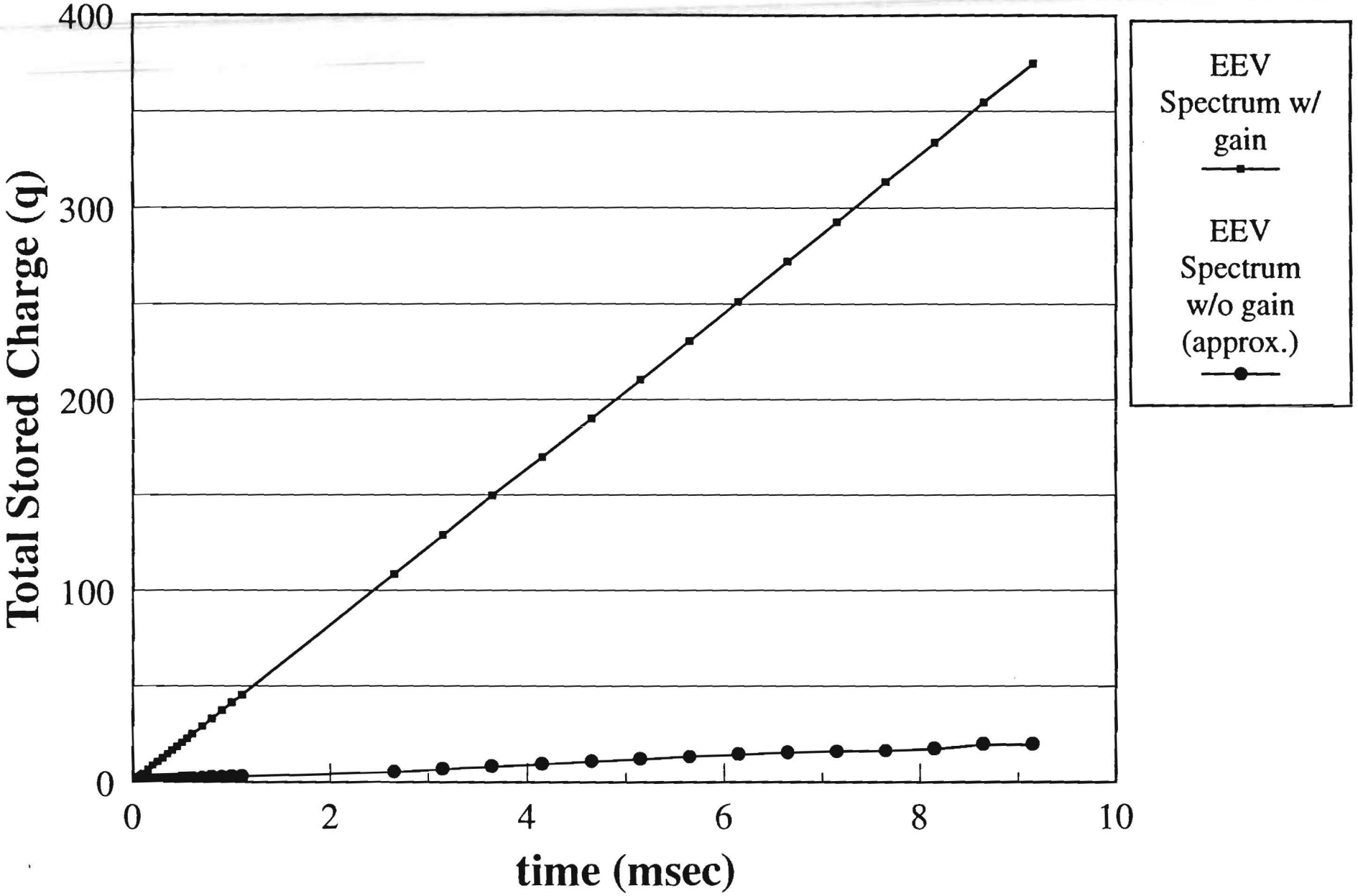

Fig 6. Total Stored Charge for Reach-Through APD Structure

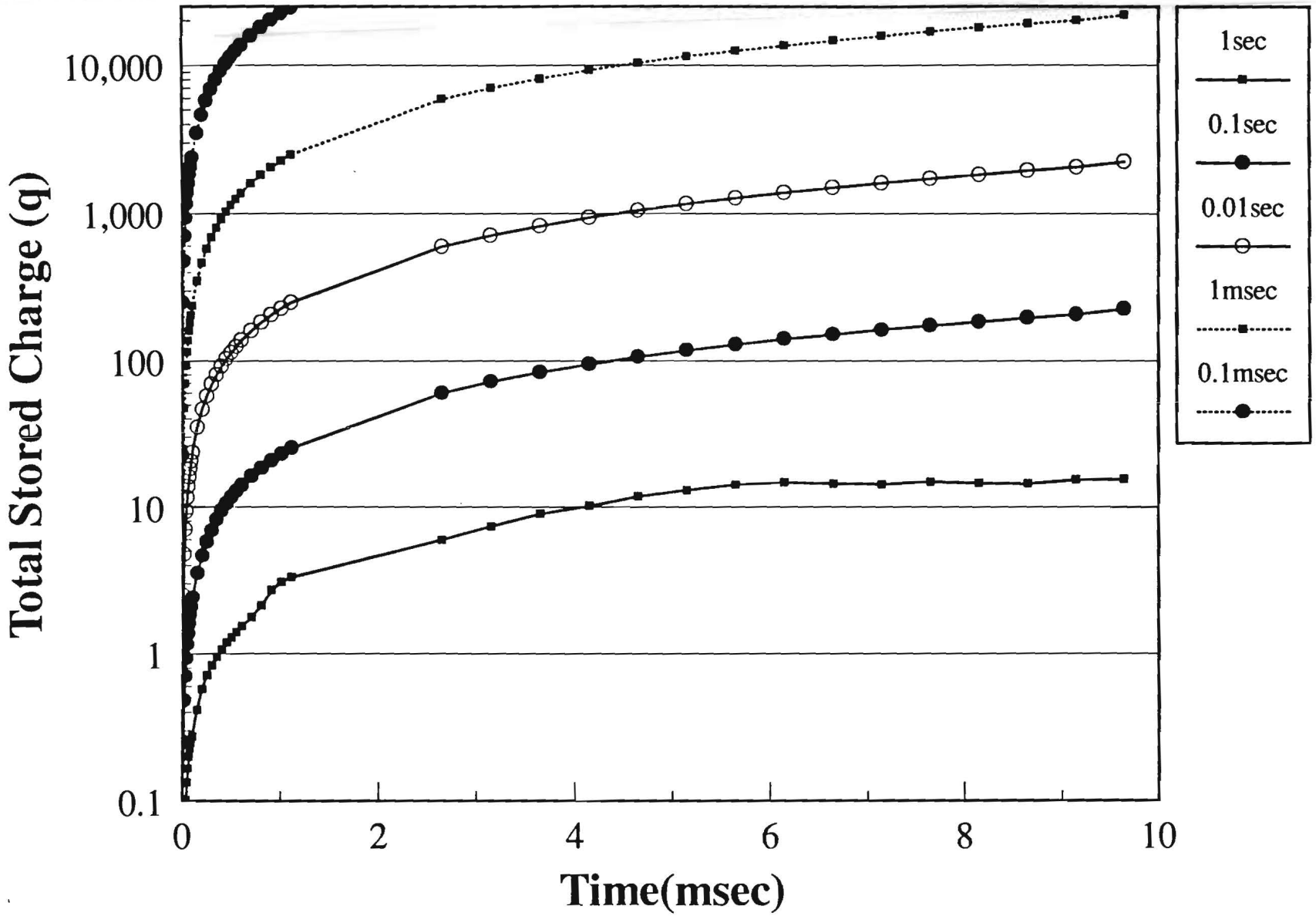

Fig 7. Total Stored Charge for Various SRH Generation Lifetimes

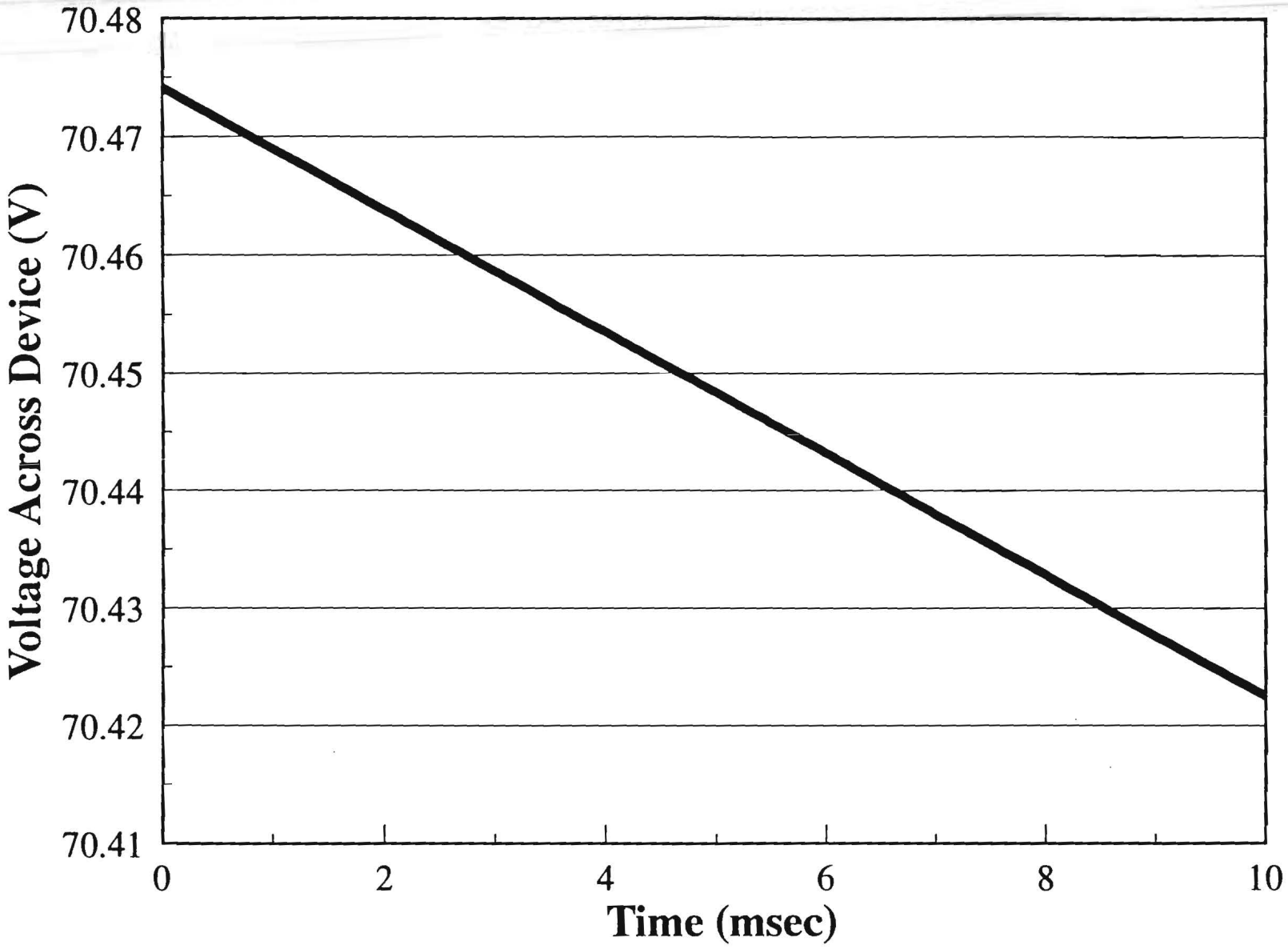

Fig 8. Reverse Recovery of Reach Through APD Structure

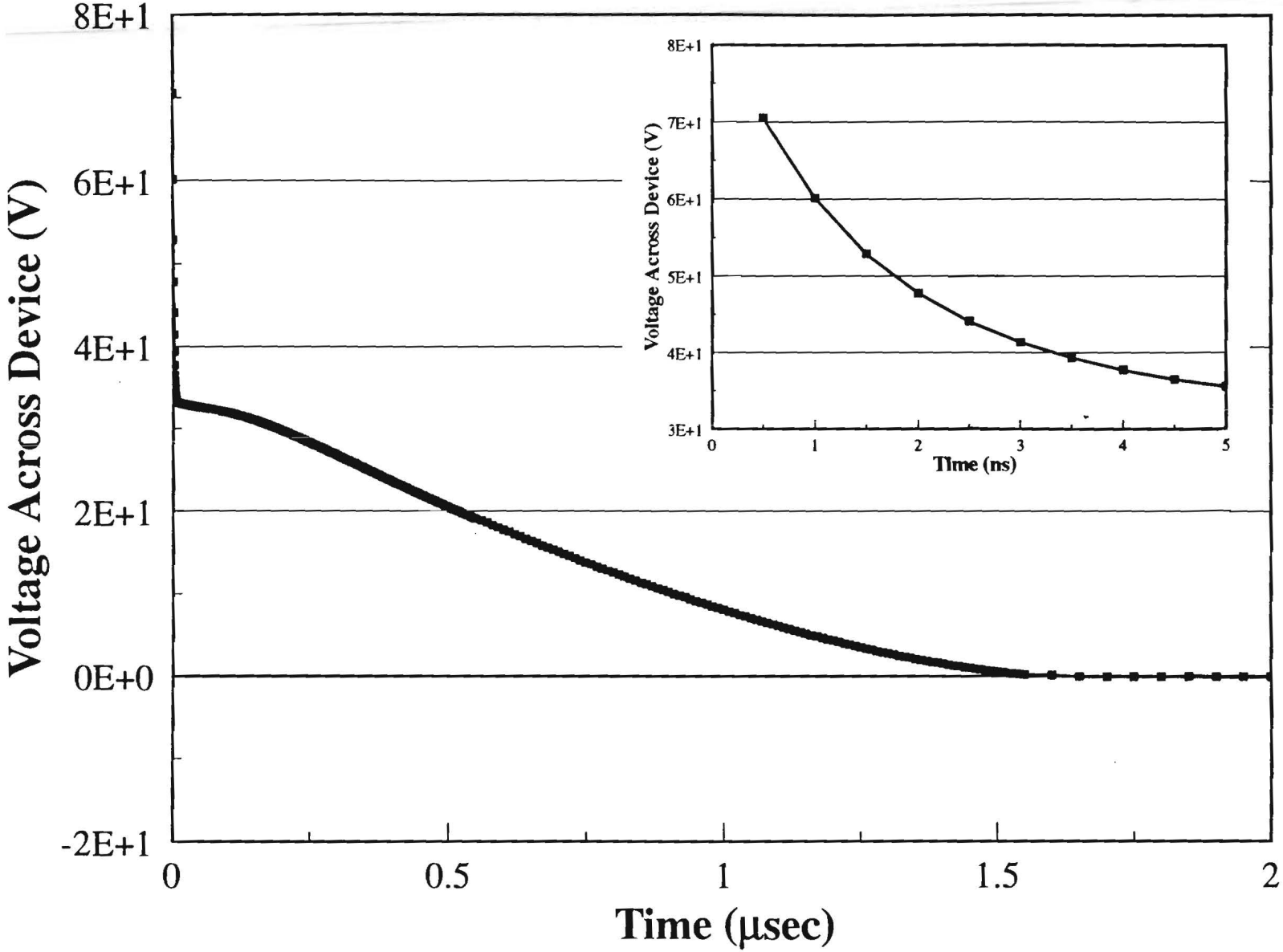

Fig 9. Reverse Recovery of Reach Through APD Structure